

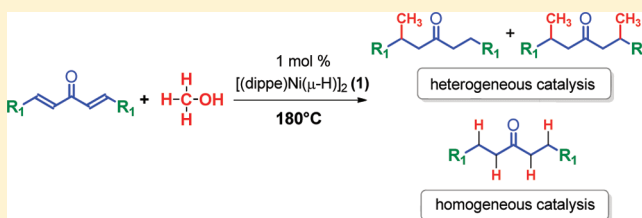
# Nickel-Catalyzed Alkylation and Transfer Hydrogenation of $\alpha,\beta$ -Unsaturated Enones with Methanol

Nahury Castellanos-Blanco, Marcos Flores-Alamo, and Juventino J. García\*

Facultad de Química, Universidad Nacional Autónoma de México, Circuito Interior, Ciudad Universitaria, Mexico City 04510, Mexico

## Supporting Information

**ABSTRACT:** Complexes of the type  $[(\text{dippe})\text{Ni}]_n(\eta^2\text{-C}_w\text{C}_\beta\text{-1,4-dien-3-one})$  (dippe = 1,2-bis(diisopropylphosphino)ethane);  $n = 1, 2$ ; enone = aromatic 1,4-pentadien-3-ones) were synthesized. The “[dippe)Ni]” moiety derived from  $[(\text{dippe})\text{Ni}(\mu\text{-H})_2]$   $\eta^2$ -coordinated to the C,C double bonds of the corresponding  $\alpha,\beta$ -unsaturated enone and was fully characterized using a variety of spectroscopic techniques, for instance, single-crystal X-ray diffraction, nuclear magnetic resonance (NMR), and mass spectrometry. The complexes were assessed in a catalytic transfer hydrogenation process using methanol ( $\text{CH}_3\text{OH}$ ) as a hydrogen donor. This alcohol turned out to be a very efficient reducing and alkylating agent of 1,4-pentadien-3-ones, under neat conditions. The current methodology allowed the selective reduction of C=C bonds in  $\alpha,\beta$ -unsaturated enones to yield enones and saturated ketones by a homogeneous catalytic pathway, whereas by a heterogeneous pathway, the process leads to the formation of mono- and dimethylated ketones. In the latter case, the occurrence of nickel nanoparticles in the reaction media was found to participate in the catalytic alkylation of such dienones.



## 1. INTRODUCTION

The catalytic transfer hydrogenation of  $\alpha,\beta$ -unsaturated carbonyl compounds is an important methodology in synthetic organic chemistry. This allows functionalization of the conjugated system present in these entities, and modification of some of its properties, for instance, the potential Michael acceptor activity that promotes the formation of toxic compounds with mutagenic and carcinogenic activity.<sup>1a,b</sup> In the second half of the 20th century, new protocols have been established for the hydrogenation of  $\alpha,\beta$ -unsaturated ketones, esters, or aldehydes,<sup>2a,b</sup> with the aim of avoiding the use of hazardous hydrogen gas and employing some simple molecules as hydrogen sources instead; the use of alcohols,<sup>3a-e,6b</sup> hydrosilanes,<sup>4a,c,5b</sup>  $\text{Et}_3\text{N}\cdot\text{HCl}$ ,<sup>6a</sup> or  $\text{HCOOH}$ <sup>8b</sup> is oftentimes preferred. This type of transformation has been possible through the use of catalysts based on transition metals, such as iridium,<sup>3b</sup> palladium,<sup>5a,b</sup> titanium,<sup>6a,b</sup> rhodium,<sup>7a,b</sup> or ruthenium,<sup>8a-c</sup> and a variety of ancillary ligands, including phosphines,<sup>3a-c,5,7b,8a</sup> cyclopentadienyl,<sup>6a,b,7a</sup> or TsEN (TsEN = *N*-(*p*-toluenesulfonyl)-1,2-ethylenediamine).<sup>7a</sup> The reduction using simple organic molecules as hydrogen donors in the presence of a catalyst makes the hydrogenation process safer and environmentally friendly.

Recent reports on the use of short-chain alcohols for the reduction of  $\alpha,\beta$ -unsaturated ketones have been documented. Regularly, ethanol and isopropanol are preferred because these alcohols are an easily accessible, economic, clean, and safe source of hydrogen.<sup>3a,c,10</sup> Comparatively, methanol is less frequently used in this kind of process, despite being cheap and more readily available than the others mentioned above. It also

contains an important amount of potentially usable hydrogen, and its use as a reducing agent is attractive in some atom economical processes.<sup>9a-d</sup> These alcohols and some other methanol derivatives have been efficiently used in the reduction of dienones in the presence of homogeneous catalysts containing Ru,<sup>3a</sup> Ir,<sup>3b</sup> and Pd,<sup>3c</sup> or heterogeneous catalysts using nickel nanoparticles.<sup>11a</sup>

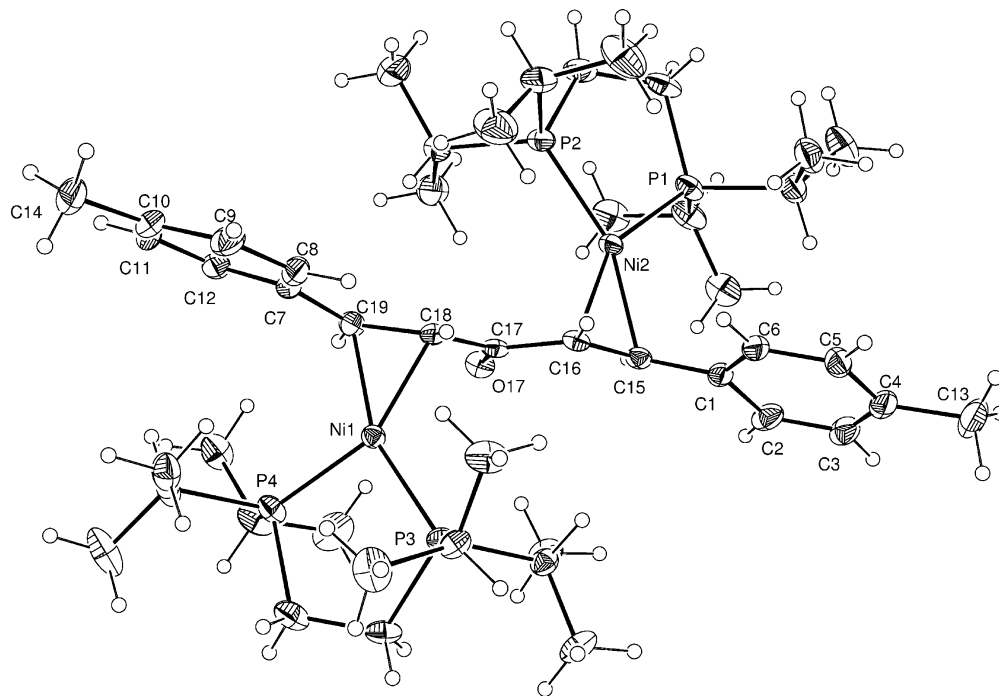
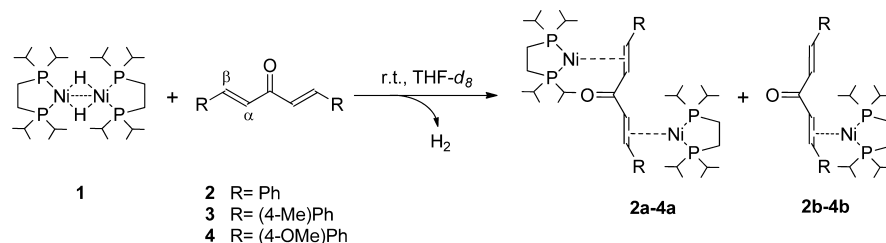
Among the reported methods using other simple molecules for dienone reduction, worthy of mention is the work by Hayashi and co-workers,<sup>12</sup> who have reported the use of the complex  $[\{\text{Ir}(\text{OH})(\text{COD})\}_2]$  (COD: cyclooctadiene) in  $\text{H}_2\text{O}$ , to efficiently yield the addition of 1,6-aryl boronic acids to dienones, with the further use of a palladium-catalyzed hydrogenation being necessary to give saturated ketones.

On the other hand, it is known that alcohols, such as ethanol and isopropanol, can also participate as alkylating agents by a heterogeneous catalytic process involving nickel nanoparticles.<sup>11a,b</sup> Recently, such nanoparticles have been used in the  $\alpha$ -alkylation of ketones, producing water as the only byproduct of the reaction.<sup>19</sup> However, these processes have not been yet documented for the alkylation of  $\alpha,\beta$ -unsaturated enones.

Feringa and co-workers reported recently a homogeneous system involving the conjugate addition of diethylzinc to symmetrical dienones, catalyzed by an in situ generated copper-phosphoramidite complex<sup>13</sup> to yield the selective activation of the C=C moiety instead of the C=O bond. According to the authors, the dienone functionalization

Received: October 23, 2011

Published: January 10, 2012

Scheme 1. Formation of Mono- and Dinuclear Complexes,  $[(\text{dippe})\text{Ni}]_n(\eta^2\text{-C}_\omega\text{C}_\beta\text{-enone})$ 

**Figure 1.** ORTEP drawing of **3a**,  $[(\text{dippe})\text{Ni}]_2(\eta^2\text{-C}_\omega\text{C}_\beta\text{-C}_{19}\text{H}_{18}\text{O})$ , showing 30% probability ellipsoids. Selected bond distances (Å): C(19)–C(18) 1.425(6), C(16)–C(15) 1.404(6), Ni(2)–C(15) 2.011(4), Ni(2)–C(16) 1.986(4), Ni(1)–C(19) 1.975(4), Ni(1)–C(18) 1.984(6). Selected bond angles (deg): C(18)–Ni(1)–C(19) 42.20(18), C(18)–Ni(1)–P(4) 152.26(14), C(19)–Ni(1)–P(4) 110.43(14), C(18)–Ni(1)–P(3) 115.21(14), C(19)–Ni(1)–P(3) 157.12(14), P(4)–Ni(1)–P(3) 92.36(5), C(16)–Ni(2)–C(15) 41.12(18), C(16)–Ni(2)–P(1) 150.69(14), C(15)–Ni(2)–P(1) 109.88(13), C(16)–Ni(2)–P(2) 117.18(13), C(15)–Ni(2)–P(2) 157.70(14), P(1)–Ni(2)–P(2) 92.08(6).

resulted in the 1,4-addition of the alkyl-organometallic reagent to produce monoalkyl-enones in good yields and with high enantioselectivities.

Herein, we would like to report the use of a catalytic precursor using a nonexpensive metal operating in two catalytic processes, homogeneous and heterogeneous, and the use of a primary alcohol as a hydrogen source, solvent, and alkylating agent.

## 2. RESULTS AND DISCUSSION

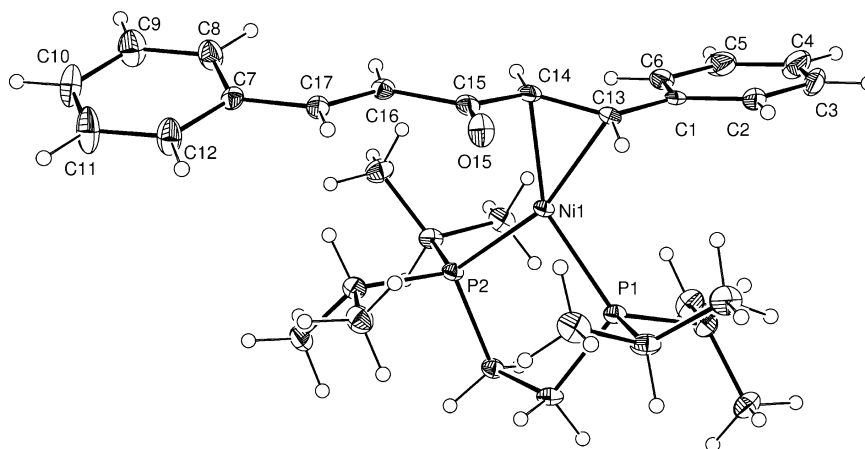
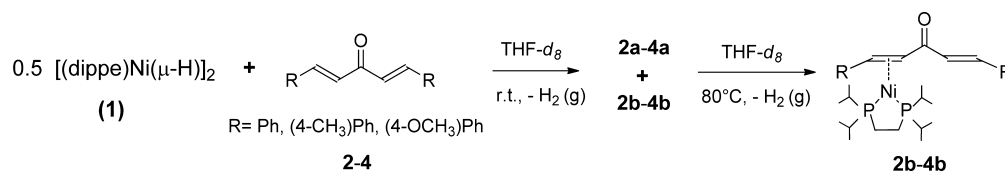
**2.1. Reactivity of  $[(\text{dippe})\text{Ni}(\mu\text{-H})]_2$  **1** with Symmetrical Dienones.** The reaction of the hydride dimer  $[(\text{dippe})\text{Ni}(\mu\text{-H})]_2$  with symmetrical dienones in  $\text{THF-}d_8$  was immediate at room temperature, and a color change from dark red to brown along with the evolution of  $\text{H}_2$  was always observed (Scheme 1).

According to Scheme 1, complexes **2a–4a** were produced as the main products by using 1 equiv of dienone per 1 equiv of complex **1**. The  $^{31}\text{P}\{^1\text{H}\}$  NMR spectrum displays two broad systems of doublet of doublets between 72 and 75 ppm with P–P coupling constants in the range of 56–59 Hz, characteristic of  $^2J_{\text{P-P}}$  in nickel(0) complexes with diphosphine

ligands.<sup>14a,b</sup> The  $^{13}\text{C}\{^1\text{H}\}$  NMR spectra are in agreement with  $\eta^2\text{-C}_\omega\text{C}_\beta$  coordination of enones to  $\text{Ni}^0$ ; key signals for the coordinated carbons are displayed between 61 and 49 ppm, at high field from their positions in the corresponding free ligand (originally, as singlets in the range of 130–150 ppm), with  $^2J_{\text{C-P}} = 13.5$  and  $^2J_{\text{C-P}} = 19.5$  Hz. The carbonyl signals for compounds **2a–4a** are slightly shifted to low field with respect to the signals for the free dienones ( $\delta$  187–188), showing singlets in the region of 190–193 ppm. The  $^1\text{H}$  NMR spectra of dinuclear complexes **2a–4a** are also in agreement with the  $\eta^2\text{-C}_\omega\text{C}_\beta$  coordination to nickel(0), since resonances for the olefinic protons in the complexes **2a–4a** appear shifted to high field in the range of 4.35–4.50 ppm, while the olefinic protons of free dienones resonate between 7.1 and 7.7 ppm.

A 1:1 mixture of dienone **2** and complex **1** in toluene- $d_8$  was heated gradually, increasing the temperature from 25 to 120 °C for 10 days. The  $^{31}\text{P}\{^1\text{H}\}$  NMR spectrum at 120 °C shows the signals assigned to the dinuclear complex **2a** and two small singlets assigned to  $[(\text{dippe})_2\text{Ni}]$ ,  $\delta$  50.2 and free diphosphine dippe,  $\delta$  7.3.<sup>14a,16</sup> This behavior is similar for dienones **3** and **4**.

Suitable crystals for single-crystal X-ray studies for compounds **3a** and **4a** were grown from a concentrated

Scheme 2. Formation of Mononuclear  $[(\text{dippe})\text{Ni}(\eta^2\text{-C}_\alpha\text{C}_\beta\text{-1,4-pentadien-3-one})]$  Complexes

**Figure 2.** ORTEP drawing of **2b**,  $[(\text{dippe})\text{Ni}(\eta^2\text{-C}_\alpha\text{C}_\beta\text{-C}_{17}\text{H}_{14}\text{O})]$ , showing 30% probability ellipsoids. Selected bond distances (Å): C(13)–C(14) 1.417(3), C(14)–C(15) 1.436(3), C(16)–C(17) 1.323(3), C(14)–Ni(1) 1.982(2), Ni(1)–P(1) 2.1538(6), Ni(1)–P(2) 2.1726(6). Selected bond angles (deg): C(14)–Ni(1)–P(1) 148.06(7), C(13)–Ni(1)–P(1) 107.25(8), C(14)–Ni(1)–P(2) 119.67(7), C(13)–Ni(1)–P(2) 159.72(8), P(1)–Ni(1)–P(2) 92.11(2).

solution in THF- $d_8$  at low temperature. The ORTEP representations for the dinuclear complexes **3a** and **4a** are shown in Figure 1 and the Supporting Information, respectively; these confirmed the structure proposed for symmetrical dienone complexes. For **3a**, in the asymmetric unit, each of the two metal nickel centers is coordinated to two phosphorus of the dippe ligand and  $\eta^2\text{-C}_\alpha\text{C}_\beta$  bonds C15–C16 and C18–C19 as expected, compared to the free dienone (1.332(3) Å).<sup>15</sup> The two metal moieties,  $[(\text{dippe})\text{Ni}]$ , are arranged in a mutually trans position with respect to the plane of ligand; each metal center has a slightly distorted trigonal-planar geometry with an rms deviation of 0.0051 and 0.0058 Å in the square plane P(3)/P(4)/centroid:C(18)–C(19) with deviations Ni(1) –0.008(3), P(3) –0.002(1), P(4) 0.002(1), centroid:C(18)–C(19) 0.003(1)° from the least-squares plane  $[10.958(13)x - 7.651(24)y - 9.529(54)z = 4.076(11)]$  and P(1)/P(2)/centroid:C(15)–C(16) with deviations Ni(2) –0.010(3), P(1) 0.002(1), P(2) 0.002(1), centroid:C(15)–C(16) 0.004(1)° from the least-squares plane  $[13.118(18)x + 5.142(24)y - 5.830(59)z = 9.162(26)]$  for Ni(1) and Ni(2) metallic centers, respectively. The planarity of the  $\eta^2\text{-C}_\alpha\text{C}_\beta$ -bis(4-methyl styryl)ketone ligand (rms deviation of fitted atoms = 0.2046 Å) is significantly affected by the coordination to nickel(0) atoms. In the supramolecular network, the intermolecular contacts of van der Waals type C–H...O and C–H...C with  $R_2^1(7)$  motif for C24–H...O(17)...H–C25 and  $D$  motif for C28–H...C5 mainly lead to infinite chains aligned with the  $a$  axis.

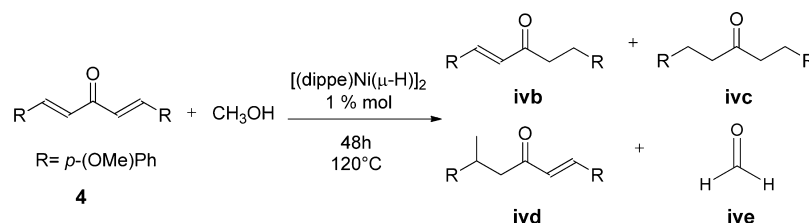
Additionally, dinuclear complexes **2a–4a** were characterized by EI<sup>+</sup>-MS, and in all cases, the corresponding molecular ion was observed in agreement with the expected  $m/z$  ratio (see the Experimental Section).

On using 0.5 equiv of complex **1** per 1 equiv of  $\alpha,\beta$ -unsaturated enones (**2–4**), the expected dinuclear complexes

**2a–4a** were observed along with the mononuclear complexes **2b–4b** depicted also in Scheme 1. Complexes **2a–4a** can be converted completely to **2b–4b** by heating at 80 °C for 1 day in THF- $d_8$  (Scheme 2).

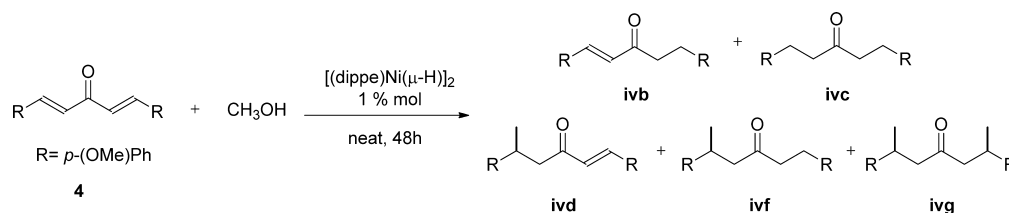
Similar to complexes **2a–4a**, the <sup>1</sup>H NMR spectra for mononuclear **2b–4b** complexes display a set of olefinic protons located at  $\delta$  5.9 and 5.6, shifted to high field with respect to the signals for free ligands ( $\delta$  7.1–7.7); these signals integrate for two protons and were assigned to the  $\eta^2\text{-C}_\alpha\text{C}_\beta$  coordination in mononuclear complexes. The <sup>31</sup>P{<sup>1</sup>H} characteristic signals for complexes **2b–4b** appear as two doublets located at  $\delta$  75.5 and 77.5 generated by two nonequivalent phosphorus coordinated to a nickel center, with  $J_{\text{P-P}} = 42\text{--}44$  Hz.

Complexes **2b–4b** were unequivocally characterized by single-crystal X-ray diffraction, and the corresponding ORTEP representation for the mononuclear complex **2b** is shown in Figure 2. The asymmetric unit of **2b** consists of the  $\eta^2$ -dibenzylideneacetone coordinated through one  $\text{C}_\alpha\text{C}_\beta$  bond to the Ni(0) fragment,  $[(\text{dippe})\text{Ni}]$ . As expected, the structure shows a lengthening for the  $\eta^2$ -coordinated  $\text{C}_\alpha\text{C}_\beta$  bond (1.417(3) Å) compared with the free ligand  $\text{C}_\alpha\text{C}_\beta$  bond (1.323(3) Å) due to the bonding to nickel, with a dihedral angle of 80.62° between the dienone ligand and the NiP2 planes. The tetracoordinate complex **2b** shows a slightly distorted trigonal-planar geometry with an rms deviation of fitted atoms = 0.0061 Å in the square plane P(1)/P(2)/centroid:C(13)–C(14) with deviations Ni(1) –0.010(4), P(1) 0.002(1), P(2) 0.003(1), centroid:C(13)–C(14) 0.004(1)° from the least-squares plane  $[10.163(39)x - 3.324(17)y - 13.513(33)z = 6.688(54)]$ . The planarity of the  $\eta^2\text{-C}_\alpha\text{C}_\beta$ -bis(4-methyl styryl)ketone ligand (rms deviation of fitted atoms = 0.2011 Å) is slightly affected by the coordination to the nickel(0) atom. In the crystal packing, there is one intermolecular contact of the type C–H...O [2.34(3) Å]

Table 1. Catalytic Hydrogenation of Di(*p*-methoxybenzylidene) Acetone Using MeOH as a Hydrogen Donor<sup>a</sup>

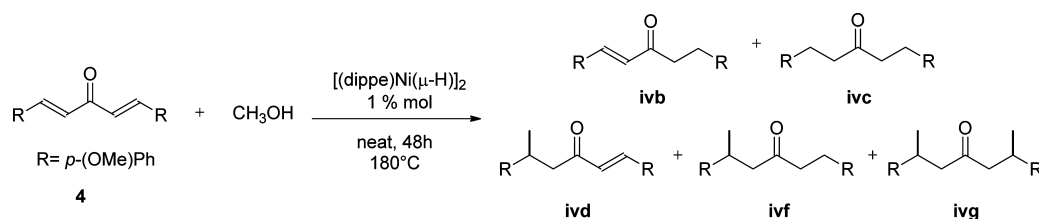
| entry | solvent  | conv (%) | yield (%) <sup>b</sup> |     |     |
|-------|----------|----------|------------------------|-----|-----|
|       |          |          | ivb                    | ivc | ivd |
| 1     | toluene  | 0        |                        |     |     |
| 2     | THF      | 5        | 5                      | 0   | 0   |
| 3     | methanol | 47       | 31                     | 3   | 13  |

<sup>a</sup>All reactions were made in a stainless steel Parr reactor using 10 mL of solvent and 5 mL of methanol. A molar proportion of 1:100 of [(dippe)Ni(μ-H)]<sub>2</sub> and di(*p*-methoxybenzylidene) acetone, respectively, was used. <sup>b</sup>All yields were measured by GC-MS.

Table 2. Effect of the Temperature in the Catalytic Hydrogenation of Di(*p*-methoxybenzylidene) Acetone Using MeOH as a Hydrogen Source<sup>a</sup>

| entry | T (°C) | conv (%) | yield (%) <sup>b</sup> |     |     |     |     |
|-------|--------|----------|------------------------|-----|-----|-----|-----|
|       |        |          | ivb                    | ivc | ivd | ivf | ivg |
| 1     | 90     | 0.7      | 0.7                    | 0   | 0   | 0   | 0   |
| 2     | 120    | 47       | 31                     | 3   | 13  | 0   | 0   |
| 3     | 150    | 93       | 47                     | 19  | 27  | 0   | 0   |
| 4     | 180    | 100      | 0                      | 18  | 0   | 76  | 6   |

<sup>a</sup>All reactions were carried out in a stainless steel Parr reactor using 15 mL of methanol. A molar proportion of 1:100 of [(dippe)Ni(μ-H)]<sub>2</sub> and di(*p*-methoxybenzylidene) acetone, respectively, was used. <sup>b</sup>All yields were quantified by GC-MS.

Table 3. Mercury Drop Experiment: Heterogeneous Process<sup>a</sup>

| entry | conv (%) | Hg (drops) | yield (%) <sup>b</sup> |     |     |     |     |
|-------|----------|------------|------------------------|-----|-----|-----|-----|
|       |          |            | ivb                    | ivc | ivd | ivf | ivg |
| 1     | 100      | 0          | 0                      | 0   | 18  | 76  | 6   |
| 2     | 100      | 3          | 0                      | 54  | 6   | 40  | 0   |

<sup>a</sup>All reactions were carried out in a stainless steel Parr reactor using 15 mL of methanol. A molar proportion of 1:100 of [(dippe)Ni(μ-H)]<sub>2</sub> and di(*p*-methoxybenzylidene) acetone, respectively, was used. <sup>b</sup>All yields were quantified by GC-MS.

mainly. This interaction leads to infinite chains aligned with the *a* axis.

**2.2. Catalytic Transfer Hydrogenation of Symmetrical Dienones Using Methanol as a Hydrogen Donor.** Considering that dinuclear complexes **2a–4a** and mononuclear **2b–4b** exhibited  $\eta^2$ -coordination of  $C_\alpha=C_\beta$  bonds to nickel(0) and that the resulting complexes turned out to be thermally stable, some catalytic transfer hydrogenation experiments were assayed using a variety of solvents and temperatures for the

different  $\alpha,\beta$ -unsaturated enones. These experiments were assessed using catalyst precursor **1** in low loads (1% mol), dienone **4**, and MeOH as a hydrogen source. Selected results are summarized in Table 1. The use of solvents, such as toluene and THF (entries 1 and 2), showed a poor conversion. However, conversion was improved with the use of methanol as a reagent and solvent (entry 3), since **4** was partially reduced to the corresponding dienone (**ivb**) and completely reduced to

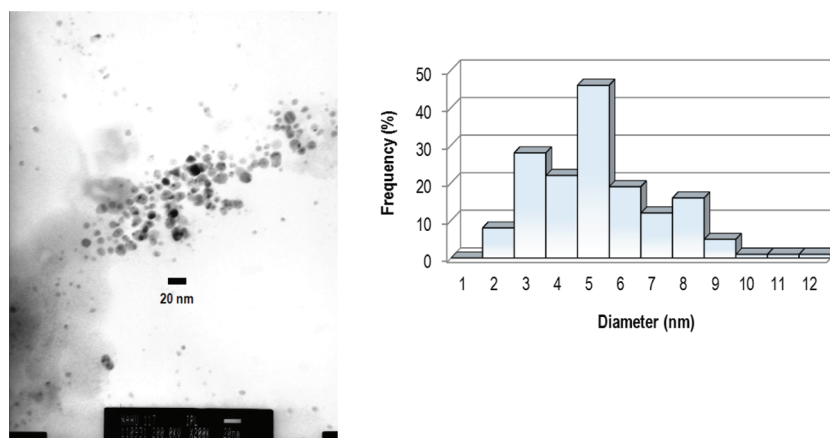
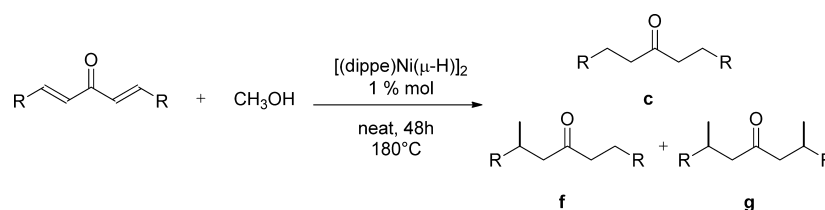


Figure 3. TEM image for the sample of entry 1 (Table 3) and size distribution of the Ni nanoparticles.

Table 4. Catalytic Hydrogenation of Aromatic Dienones Using MeOH<sup>a</sup>



| entry | R                                | conv (%) | yield (%) <sup>b</sup> |     |    |
|-------|----------------------------------|----------|------------------------|-----|----|
|       |                                  |          | c                      | f   | g  |
| 1     | Ph                               | 100      | 0                      | 100 | 0  |
| 2     | Ph( <i>p</i> -CH <sub>3</sub> )  | 100      | 0                      | 82  | 18 |
| 3     | Ph( <i>p</i> -OCH <sub>3</sub> ) | 100      | 18                     | 76  | 6  |

<sup>a</sup>All reactions were carried out in a stainless steel Parr reactor using 15 mL of methanol. A molar proportion of 1:100 of [(dippe)Ni( $\mu$ -H)]<sub>2</sub> and di(*p*-methoxybenzylidene) acetone, respectively, was used. <sup>b</sup>All yields were quantified by GC-MS.

the saturated ketone (**ivc**). Noteworthy, a monomethylated dienone (**ivd**) was detected by GC-MS.

The use of methanol as a hydrogen source is well-known,<sup>17</sup> being oxidized to formaldehyde (**ive**) during the reaction.<sup>9d</sup> However, its use as an alkylating agent is less common; therefore, **ivd** is an unexpected product for this homogeneous catalytic process. Closely related reactions have been documented by Yus et al., in which primary alcohols, such as ethanol and isopropanol, can be used as alkylating agents in a heterogeneous catalytic reaction using nickel nanoparticles.<sup>11a,b</sup> Also, these nanoparticles have been used in the  $\alpha$ -alkylation of ketones recently, producing water as the only byproduct of the reaction.<sup>19</sup> These results prompted us to screen the observed reactivity toward nickel nanoparticle formation (vide infra).

On raising the temperature for the same reaction to 150 °C, an improvement in conversion was obtained (Table 2), and consequently, an increase in yield for the hydrogenation and alkylation products was observed. With a further rise to 180 °C, two new alkylation products were detected in good yields by GC-MS: the monomethylated (76%, **ivf**) and the dimethylated ketone (6%, **ivg**) (see Table 2).

To investigate the occurrence of nickel nanoparticles in the reaction media, a mercury drop test was made, adding three drops of elemental mercury into the reaction vessel. A significant decrease in the formation of alkylation products (**ivf**–**ivg**) and an increase of the hydrogenation product (**ivc**) were observed (see Table 3) as compared with the mercury-free reaction (entry 1), allowing us to conclude that

heterogeneous Ni(0) was involved in the production of alkylated products. Further studies on this reaction allowed us to establish the formation and participation of Ni nanoparticles, which were characterized by TEM (Figure 3). Here, an average size of 5 nm for the nanoparticles was found in a typical sample (from entry 1, Table 3).

To extend the observed reactivity between methanol and  $\alpha,\beta$ -unsaturated enones, the methylation process was applied to other aromatic dienones also used in this work (see Table 4).

As found for **4**, the monomethylation product **f** was preferred in all the reactions shown in Table 4, being the only product in the case in which R = Ph. Noteworthy, the substitution in the aromatic ring with electron-releasing groups (entries 2 and 3) yielded mixtures of mono- and dimethylated ketones.

### 3. CONCLUSIONS

The selective C <sub>$\alpha$</sub> =C <sub>$\beta$</sub>  bond coordination and activation in  $\alpha,\beta$ -unsaturated enones, using a Ni(0) complex with electron-rich P-donor ancillary ligands was found. The reactions that took place yielded mononuclear and dinuclear complexes of the general formula [(dippe)Ni]<sub>*n*</sub>( $\eta^2$ -C <sub>$\alpha$</sub> =C <sub>$\beta$</sub> -enone)]. A tandem catalytic hydrogenation and alkylation of  $\alpha,\beta$ -unsaturated enones with methanol was found in a homogeneous/heterogeneous process involving homogeneous nickel(0) complexes and nickel nanoparticles, respectively. The current report offers the use of CH<sub>3</sub>OH also as an alkylating agent, using a nonexpensive metal, such as nickel, as a catalyst. Current studies are underway

to extend the scope of this reaction to other alcohols and P-donor ligands.

#### 4. EXPERIMENTAL SECTION

Unless otherwise noted, all manipulations were performed using standard Schlenk techniques in an inert-gas/vacuum double manifold or under an argon atmosphere (Praxair 99.998) in an MBraun glovebox (<1 ppm H<sub>2</sub>O and O<sub>2</sub>). All liquid reagents were purchased in reagent grade and were degassed before use. All  $\alpha,\beta$ -unsaturated enones were purchased from Aldrich and were stored in a glovebox for their further use. The nickel(I) dimer, [(dippe)Ni( $\mu$ -H)]<sub>2</sub> (**1**), was prepared from an *n*-hexanes slurry of [(dippe)NiCl<sub>2</sub>]<sup>18a</sup> using Super-Hydride (LiHBEt<sub>3</sub>), according to the reported procedure.<sup>18b</sup> The solvents were dried using standard techniques and stored in the glovebox before use. Deuterated solvents were purchased from Cambridge Isotope Laboratories and were stored under 4 Å molecular sieves for 24 h before use. NMR spectra were recorded at room temperature on a 300 MHz Varian Unity spectrometer unless otherwise noted. <sup>1</sup>H NMR spectra ( $\delta$ , parts per million) are reported relative to the residual protio-solvent. <sup>13</sup>C{<sup>1</sup>H} spectra are referred to the characteristic carbon signal of each solvent. <sup>31</sup>P{<sup>1</sup>H} NMR chemical shifts ( $\delta$ , parts per million) are reported relative to external 85% H<sub>3</sub>PO<sub>4</sub>. <sup>1</sup>H and <sup>13</sup>C{<sup>1</sup>H} NMR spectra of the reduction products were obtained in CDCl<sub>3</sub>. An Oxford Diffraction Gemini "A" diffractometer with a CCD area detector ( $\lambda_{\text{Mo K}\alpha}$  = 0.71073 Å) was used for X-ray structure determinations. Catalytic experiments were carried out in a 100 mL stainless steel Parr, T315SS reactor. Elemental analyses (EAs) were also performed by USAI-UNAM using a PerkinElmer microanalyzer 2400. EAs of pure compounds showed variable inconsistencies due to their high oxygen sensitivity and were not reported; however, all of them display satisfactory MS-EI<sup>+</sup>. Mass spectrometry determinations (MS-EI<sup>+</sup>) of pure compounds were performed by USAI-UNAM using a Thermo-Electron DFS.

**4.1. Preparation of [(dippe)Ni]<sub>2</sub>( $\eta^2$ -C<sub>w</sub>C<sub>\beta</sub>-Dibenzylideneacetone), (**2a**).** The reaction of dibenzylideneacetone **2** (0.047 mmol, 0.0109 g) with **1** (0.046 mmol, 0.030 g) in THF-*d*<sub>8</sub> (1 mL) yielded a dinuclear nickel(0) complex [(dippe)Ni]<sub>2</sub>( $\eta^2$ -C<sub>w</sub>C<sub>\beta</sub>-dibenzylideneacetone) (**2a**). Immediate effervescence due to reductive elimination of H<sub>2</sub> was observed during mixing. The resulting solution was analyzed by NMR spectroscopy: <sup>31</sup>P{<sup>1</sup>H} NMR (121.32 MHz, THF-*d*<sub>8</sub>, r.t.):  $\delta$  = 75.0 (dd, *J*<sub>P-P</sub> = 56.5 Hz, *J*<sub>C-P</sub> = 8.3 Hz),  $\delta$  = 72.4 (dd, *J*<sub>P-P</sub> = 57.02 Hz, *J*<sub>C-P</sub> = 8.28 Hz). <sup>13</sup>C NMR (75.36 MHz, THF-*d*<sub>8</sub>, r.t.):  $\delta$  = 190.86 (s, 1C, <sup>13</sup>C=O), 150.211 (s, 4C, C-aromatic), 128.59 (s, 5C, 9C, CH-aromatic), 125.57 (s, 6C, 8C, CH-aromatic), 121.65 (s, 7C, C-aromatic), 60.4 (d, *J*<sub>C-P</sub> = 10.70 Hz, 3C, CH-olefinic), 50.4 (d, *J*<sub>C-P</sub> = 19.59 Hz, 2C, CH-olefinic), 26.90–17.44 (m, *i*Pr CH, CH<sub>2</sub>, CH<sub>3</sub>). <sup>1</sup>H NMR (300 MHz, THF-*d*<sub>8</sub>, r.t.):  $\delta$  = 7.13 (d, *J*<sub>H-H</sub> = 7.2 Hz, 5H, 9H, aromatics), 6.98 (t, *J*<sub>H-H</sub> = 7.2 Hz, 6H, 8H, aromatics), 6.75 (t, *J*<sub>H-H</sub> = 7.2 Hz, 7H, aromatics), 4.48 (m, *J*<sub>H-P</sub> = 3 Hz, 2H, CH-olefinic), 2.29–0.34 (m, *i*Pr CH, CH<sub>2</sub>, CH<sub>3</sub>). Molecular ion mass spectrometry: [MS-EI<sup>+</sup>, *m/z* (%) 874 (2.2%)].

**4.2. Preparation of [(dippe)Ni( $\eta^2$ -C<sub>w</sub>C<sub>\beta</sub>-Dibenzylideneacetone), (**2b**).** The reaction of dibenzylideneacetone **2** (0.0427 mmol, 0.010 g) with **1** (0.0213 mmol, 0.030 g) in THF-*d*<sub>8</sub> (1 mL) yielded a mononuclear nickel(0) complex [(dippe)Ni( $\eta^2$ -C<sub>w</sub>C<sub>\beta</sub>-dibenzylideneacetone)] (**2b**). The reaction mixture was prepared in an NMR tube equipped with a J. Young valve and was heated in an oil bath at 80 °C during 21 h. Slow evaporation of THF-*d*<sub>8</sub> at –26 °C in the drybox allowed the crystallization of the pure product. The resulting solution was analyzed by NMR spectroscopy: <sup>31</sup>P{<sup>1</sup>H} NMR (121.32 MHz, THF-*d*<sub>8</sub>, r.t.):  $\delta$  = 77.54, 75.5 (dd, *J*<sub>P-P</sub> = 42.49 Hz). <sup>1</sup>H NMR (300 MHz, THF-*d*<sub>8</sub>, r.t.):  $\delta$  = 7.39 (d, *J*<sub>H-H</sub> = 7.2 Hz, 5H, 9H, aromatic), 7.16 (t, *J*<sub>H-H</sub> = 7.2 Hz, 6H, 8H, aromatic), 6.93 (t, *J*<sub>H-H</sub> = 7.2 Hz, 7H, aromatic), 5.89 (d, *J*<sub>H-P</sub> = 3 Hz, 3H, CH-olefinic), 5.74 (d, *J*<sub>H-P</sub> = 3 Hz, 2H, CH-olefinic), 2.30–0.34 (m, *i*Pr CH, CH<sub>2</sub>, CH<sub>3</sub>). [MS-EI<sup>+</sup>, *m/z* (%) 554 (0.6%)].

**4.3. Preparation of [(dippe)Ni]<sub>2</sub>( $\eta^2$ -C<sub>w</sub>C<sub>\beta</sub>-Bis(4-methyl styryl)ketone), (**3a**).** Similar to the procedure described for complex **2a**, the reaction between **1** (0.114 mmol, 0.0737 g) and bis(4-methyl styryl)ketone **3** (0.114 mmol, 0.030 g) in THF-*d*<sub>8</sub> (1 mL) yielded the

[(dippe)Ni]<sub>2</sub>( $\eta^2$ -C<sub>w</sub>C<sub>\beta</sub>-bis(4-methyl styryl)ketone)] (**3a**) complex. Slow evaporation of THF-*d*<sub>8</sub> at –26 °C in the drybox allowed the crystallization of the pure product. The resulting solution was analyzed by NMR spectroscopy: <sup>31</sup>P{<sup>1</sup>H} NMR (121.32 MHz, THF-*d*<sub>8</sub>, r.t.):  $\delta$  = 74.6 (dd, *J*<sub>P-P</sub> = 57.87 Hz, *J*<sub>C-P</sub> = 8.33 Hz),  $\delta$  = 72.6 (dd, *J*<sub>P-P</sub> = 58.11 Hz, *J*<sub>C-P</sub> = 8.13 Hz). <sup>13</sup>C{<sup>1</sup>H} NMR (75.36 MHz, THF-*d*<sub>8</sub>, r.t.):  $\delta$  = 190.57 (s, 9C, <sup>13</sup>C=O), 147.073 (s, 3C, C-aromatic), 130.37 (s, 6C, C-aromatic), 129.51 (s, 1C, 5C, CH-aromatic), 125.49 (s, 2C, 4C, CH-aromatic), 60.68 (d, *J*<sub>C-P</sub> = 13.11 Hz, 7C, CH-olefinic), 50.4 (d, *J*<sub>C-P</sub> = 19.44 Hz, 8C, CH-olefinic), 21.65 (s, *p*-CH<sub>3</sub>, 10C), 28.0–17.9 (m, *i*Pr CH, CH<sub>2</sub>, CH<sub>3</sub>). <sup>1</sup>H NMR (300 MHz, THF-*d*<sub>8</sub>, r.t.):  $\delta$  = 7.28 (d, *J*<sub>H-H</sub> = 8.1 Hz, 4H, 2H, aromatic), 6.812 (d, *J*<sub>H-H</sub> = 7.8 Hz, 5H, 1H, aromatic), 4.49 (m, *J*<sub>H-P</sub> = 3 Hz, 7H, CH-olefinic), 4.29 (m, *J*<sub>H-P</sub> = 3 Hz, 8H, CH-olefinic), 2.12 (s, 10H, H-*p*-CH<sub>3</sub>), 2.28–0.334 (m, *i*Pr CH, CH<sub>2</sub>, CH<sub>3</sub>). [MS-EI<sup>+</sup>, *m/z* (%) 904(5.0%)].

**4.4. Preparation of [(dippe)Ni( $\eta^2$ -C<sub>w</sub>C<sub>\beta</sub>-Bis(4-methyl styryl)ketone), (**3b**).** The reaction of bis(4-methyl styryl)ketone **3** (0.114 mmol, 0.030 g) with **1** (0.114 mmol, 0.0184 g) in 1 mL of THF-*d*<sub>8</sub> yielded a mononuclear nickel(0) complex [(dippe)Ni( $\eta^2$ -C<sub>w</sub>C<sub>\beta</sub>-bis(4-methyl styryl)ketone)] (**3b**). Slow evaporation of THF-*d*<sub>8</sub> at –26 °C in the drybox allowed the crystallization of the pure product. The resulting solution was analyzed by NMR spectroscopy: <sup>31</sup>P{<sup>1</sup>H} NMR (121.32 MHz, THF-*d*<sub>8</sub>, r.t.):  $\delta$  = 77.52, 75.35 (dd, *J*<sub>P-P</sub> = 42.46 Hz). <sup>1</sup>H NMR (300 MHz, THF-*d*<sub>8</sub>, r.t.):  $\delta$  = 7.58 (d, *J*<sub>H-H</sub> = 8.1 Hz, 4H, 2H, aromatic), 6.81 (d, *J*<sub>H-H</sub> = 8.1 Hz, 5H, 1H, aromatic), 5.906 (d, *J*<sub>H-P</sub> = 11.4 Hz, 7H, CH-olefinic), 5.704 (m, *J*<sub>H-P</sub> = 13.2 Hz, 8H, CH-olefinic), 2.118 (s, 10H, H-*p*-CH<sub>3</sub>), 2.009–0.328 (m, *i*Pr CH, CH<sub>2</sub>, CH<sub>3</sub>). [MS-EI<sup>+</sup>, *m/z* (%) 584 (1.7%)].

**4.5. Preparation of [(dippe)Ni]<sub>2</sub>( $\eta^2$ -C<sub>\alpha</sub>C<sub>\beta</sub>-Bis(4-methoxybenzylidene)acetone), (**4a**).** Similar to the preparation of compounds **2a** and **3a** (vide supra), the reaction between **1** (0.104 mmol, 0.0689 g) and bis(4-methoxybenzylidene)acetone **4** (0.105 mmol, 0.030 g) in THF-*d*<sub>8</sub> (1 mL) yielded the [(dippe)Ni]<sub>2</sub>( $\eta^2$ -C<sub>w</sub>C<sub>\beta</sub>-bis(4-methoxybenzylidene)acetone)] (**4a**) complex. Slow evaporation of THF-*d*<sub>8</sub> at –26 °C in the drybox allowed the crystallization of the pure product. The resulting solution was analyzed by NMR spectroscopy: <sup>31</sup>P{<sup>1</sup>H} NMR (121.32 MHz, THF-*d*<sub>8</sub>, r.t.):  $\delta$  = 74.0 (dd, *J*<sub>P-P</sub> = 59.28 Hz, *J*<sub>C-P</sub> = 8.00 Hz, *J*<sub>C-P</sub> = 7.15 Hz),  $\delta$  = 72.3 (dd, *J*<sub>P-P</sub> = 59.44 Hz, *J*<sub>C-P</sub> = 8.12 Hz, *J*<sub>C-P</sub> = 8.25 Hz). <sup>13</sup>C{<sup>1</sup>H} NMR (75.36 MHz, THF-*d*<sub>8</sub>, r.t.):  $\delta$  = 190.161 (s, 1C, <sup>13</sup>C=O), 156.081 (s, 7C, C-aromatic), 142.525 (s, 4C, C-aromatic), 126.183 (s, 6C, 8C, CH-aromatic), 114.296 (s, 5C, 9C, CH-aromatic), 61.083 (d, *J*<sub>C-P</sub> = 12.81 Hz, 3C, CH-olefinic), 49.978 (d, *J*<sub>C-P</sub> = 20.12 Hz, 2C, CH-olefinic), 55.37 (s, *p*-O-CH<sub>3</sub>, 10C), 26.88–17.47 (m, *i*Pr CH, CH<sub>2</sub>, CH<sub>3</sub>). <sup>1</sup>H NMR (300 MHz, THF-*d*<sub>8</sub>, r.t.):  $\delta$  = 6.98 (d, *J*<sub>H-H</sub> = 7.8 Hz, 5H, 9H, aromatic), 6.53 (d, *J*<sub>H-H</sub> = 7.8 Hz, 6H, 8H, aromatic), 4.36 (m, *J*<sub>H-P</sub> = 2.4 Hz, 3H, CH-olefinic), 4.25 (m, *J*<sub>H-P</sub> = 2.4 Hz, 2H, CH-olefinic), 3.50 (s, 10H, H-*p*-O-CH<sub>3</sub>), 2.20–0.327 (m, *i*Pr CH, CH<sub>2</sub>, CH<sub>3</sub>). [MS-EI<sup>+</sup>, *m/z* (%) 935(5.5%)].

**4.6. Preparation of [(dippe)Ni( $\eta^2$ -C<sub>\alpha</sub>C<sub>\beta</sub>-Bis(4-methoxybenzylidene)acetone), (**4b**).** The reaction between bis(4-methoxybenzylidene)acetone **4** (0.105 mmol, 0.030 g) and **1** (0.053 mmol, 0.0344 g) in THF-*d*<sub>8</sub> (1 mL) yielded the mononuclear nickel(0) complex [(dippe)Ni( $\eta^2$ -C<sub>w</sub>C<sub>\beta</sub>-bis(4-methoxybenzylidene)acetone)] (**4b**). Slow evaporation of THF-*d*<sub>8</sub> at –26 °C in the drybox allowed the crystallization of the pure product. The resulting solution was analyzed by NMR spectroscopy: <sup>31</sup>P{<sup>1</sup>H} NMR (121.32 MHz, THF-*d*<sub>8</sub>, r.t.):  $\delta$  = 75.0 (dd, *J*<sub>P-P</sub> = 44.03 Hz). <sup>1</sup>H NMR (300 MHz, THF-*d*<sub>8</sub>, r.t.):  $\delta$  = 7.318 (d, *J*<sub>H-H</sub> = 8.7 Hz, 4H, 2H, aromatic), 6.78 (d, *J*<sub>H-H</sub> = 8.7 Hz, 5H, 1H, aromatic), 5.89 (d, *J*<sub>H-P</sub> = 10.5 Hz, 7H, CH-olefinic), 5.643 (m, *J*<sub>H-P</sub> = 12.6 Hz, 8H, CH-olefinic), 3.727 (s, 10H, H-*p*-O-CH<sub>3</sub>), 2.033–0.799 (m, *i*Pr CH, CH<sub>2</sub>, CH<sub>3</sub>). [MS-EI<sup>+</sup>, *m/z* (%) 615 (4.5%)].

**4.7. Catalytic Transfer Hydrogenation.** A 100 mL Parr reactor was typically charged with a constant amount of **1** (1.55 × 10<sup>–3</sup> mmol, 0.001 g), and the corresponding  $\alpha,\beta$ -unsaturated ketone:bis(4-methoxybenzylidene)acetone (0.155 mmol, 0.0456 g), dissolved in methanol (15 mL). The resulting solutions were heated with vigorous stirring at the temperatures and times indicated in Tables 1 and 2, and after that time, the reactor was opened in a well-vented hood prior to

workup. Orange or yellow solutions were formed. These were filtered over Celite and analyzed by GC-MS.

**4.8. Mercury Drop Tests.** Following the procedure described in section 4.7, three drops of elemental Hg were added to the reaction mixture (entry 2, Table 3). At the end of each run, the corresponding solution was filtered and analyzed by GC-MS. The nanoparticles were characterized using a JEOL-2010 electron microscope, equipped with a lanthanum hexaboride filament, operated at an acceleration voltage of 200 kV.

**4.9. X-ray Structure Determination.** The crystals for compounds **3a–4a** and **2b–4b** were first cryoprotected using Paratone-N and mounted on glass fibers; immediately, the crystals were cooled at 130 K using a Cryojet cryostream (Oxford Cryosystems device). Diffraction data were collected on an Oxford Diffraction Gemini diffractometer with a CCD-Atlas area detector using a radiation source graphite monochromator,  $\lambda_{\text{Mo K}\alpha} = 0.71073 \text{ \AA}$ . CrysAlisPro and CrysAlis RED software packages<sup>20a</sup> were used for data collection and data integration. All data sets consisted of frames of intensity data collected with a frame width of  $1^\circ$  in  $\omega$ , a counting time of 27–30 s/frame, and a crystal-to-detector distance of 55.00 mm. The double pass method of scanning was used to exclude any noise. The collected frames were integrated by using an orientation matrix determined from the narrow frame scans. Final cell constants were determined by a global refinement; collected data were corrected for absorbance by using analytical numeric absorption correction<sup>20b</sup> using a multifaceted crystal model based on expressions upon the Laue symmetry using equivalent reflections.

Structure solution and refinement were carried out with the program(s) SHELXS97 and SHELXL97<sup>20c</sup>; for molecular graphics, the program ORTEP-3 for Windows<sup>20d</sup> was used; and to prepare material for publication, the software WinGX was used.<sup>20e</sup>

Full-matrix least-squares refinement was carried out by minimizing  $(F_o^2 - F_c^2)^2$ . All non-hydrogen atoms were refined anisotropically. H atoms attached to C atoms were placed in geometrically idealized positions and refined as riding on their parent atoms, with C–H = 0.93–1.00 Å and  $U_{\text{iso}}(\text{H}) = 1.2U_{\text{eq}}(\text{C})$ , or  $1.5U_{\text{eq}}(\text{C})$  for aromatic, methylene, methyne, and methyl groups. Crystal data and experimental details of the structure determination are listed in the Supporting Information.

## ■ ASSOCIATED CONTENT

### ● Supporting Information

Complete experimental procedures, ORTEP drawings, NMR spectra, and GC-MS determinations of all products. This material is available free of charge via the Internet at <http://pubs.acs.org>.

## ■ AUTHOR INFORMATION

### Corresponding Author

\*E-mail: [juvent@servidor.unam.mx](mailto:juvent@servidor.unam.mx).

## ■ ACKNOWLEDGMENTS

We thank CONACyT (080606) and PAPIIT-DGAPA-UNAM (IN-201010) for their financial support to this work. N.C.-B. thanks CONACyT for a graduate studies grant. Also, we thank Dr. Alma Arévalo for technical support.

## ■ REFERENCES

- (1) (a) Amslinger, S. *ChemMedChem* **2010**, *5*, 351. (b) Koleva, Y. K.; Madden, J. C.; Cronin, M.-D. *Chem. Res. Toxicol.* **2008**, *21*, 2300.
- (2) (a) Brieger, G.; Nestrick, T. J. *J. Chem. Rev.* **1974**, *74*, 567. (b) Mohan, J.; Sharma, P. *Bull. Chem. Soc. Jpn.* **2004**, *77*, 549.
- (3) (a) Sasson, Y.; Blum, J. *J. Org. Chem.* **1975**, *40*, 1887. (b) Sakaguchi, S.; Yamaga, T.; Ishii, Y. *J. Org. Chem.* **2001**, *66*, 4710. (c) Monguchi, D.; Beemelmans, C.; Hashizume, D.; Hamashima, Y.; Sodeoka, M. *J. Organomet. Chem.* **2008**, *693*, 867. (d) Magnus, P.;

Waring, M. J.; Scott, D. A. *Tetrahedron Lett.* **2000**, *41*, 9731. (e) Azua, A.; Mata, J. A.; Peris, E. *Organometallics* **2011**, *1*, 1390–1399.

(4) (a) Keinan, E.; Perez, D. *J. Org. Chem.* **1987**, *52*, 2577. (b) Mori, A.; Fujita, A.; Kajiro, H.; Nishihara, Y.; Hiyama, T. *Tetrahedron* **1999**, *55*, 4573. (c) Ojima, I.; Kogure, T. *Organometallics* **1982**, *1*, 1390–1399.

(5) (a) Otsuka, H.; Shirakawa, E.; Hayashi, T. *Chem. Commun.* **2007**, 1819. (b) Keinan, E.; Greenspoon, N. *J. Am. Chem. Soc.* **1986**, *108*, 7314.

(6) (a) Kosal, A. D.; Ashfeld, B. L. *Org. Lett.* **2010**, *12*, 44. (b) Moisan, L.; Hardouin, C.; Rousseau, B.; Doris, E. *Tetrahedron Lett.* **2002**, *43*, 2013–2015.

(7) (a) Li, X.; Li, L.; Tang, Y.; Zhong, L.; Cun, L.; Zhu, J.; Liao, J.; Deng, J. *J. Org. Chem.* **2010**, *75*, 2981. (b) Evans, D. A.; Fu, G. C. *J. Org. Chem.* **1990**, *55*, 5679.

(8) (a) Zheng, G. Z.; Chan, T. H. *Organometallics* **1996**, *14*, 70. (b) Fujii, A.; Hashiguchi, S.; Uematsu, N.; Ikariya, T.; Noyori, R. *J. Am. Chem. Soc.* **1996**, *118*, 2521. (c) Naskar, S.; Bhattacharjee, M. *Tetrahedron Lett.* **2007**, *48*, 465.

(9) (a) Olah, G. A.; Goepfert, A. K.; Prakash, S. *Beyond Oil and Gas: The Methanol Economy*; Wiley VCH: Weinheim, Germany, 2006; pp 168–176. (b) Smith, T. A.; Maitlis, P. M. *J. Organomet. Chem.* **1985**, *289*, 385. (c) Tani, K.; Iseki, A.; Yamagata, T. *Chem. Commun.* **1999**, 1821. (d) Barrios-Francisco, R.; García, J. J. *Inorg. Chem.* **2009**, *48*, 386.

(10) Tsuchiya, Y.; Hamashima, Y.; Sodeoka, M. *Org. Lett.* **2006**, *8*, 4851.

(11) (a) Alonso, F.; Riente, P.; Yus, M. *Acc. Chem. Res.* **2011**, *44*, 379. (b) Alonso, F.; Riente, P.; Yus, M. *Tetrahedron Lett.* **2008**, *64*, 1847.

(12) Nishimura, T.; Yasuhara, Y.; Hayashi, T. *Angew. Chem., Int. Ed.* **2006**, *45*, 5164.

(13) Sevesta, R.; Pizzuri, G.; Minnaard, A.; Feringa, B. *Adv. Synth. Catal.* **2007**, *349*, 1931.

(14) (a) Edelbach, B. L.; Lachiotte, R. J.; Jones, W. D. *Organometallics* **1999**, *18*, 4040. (b) Flores-Gaspar, A.; Pinedo, P.; Crestani, M.; Muñoz, M.; Morales, D.; Warsop, B.; Jones, W. D.; García, J. J. *Mol. Catal. A: Chem.* **2009**, *309*, 1.

(15) Complex **3b** is taken as a reference for the  $C_\alpha=C_\beta$  bond distance in the free ligand, due to the presence of uncoordinated olefinic bond C15–C16.

(16) (a) Edelbach, B. L.; Lachiotte, R. J.; Jones, W. D. *J. Am. Chem. Soc.* **1998**, *120*, 2843.

(17) (a) Tani, K.; Iseki, A.; Yamagata, T. *Chem. Commun.* **1999**, 1821.

(18) (a) Scott, C.; Krüger, C.; Betz, P. *Organomet. Chem.* **1990**, *387*, 113. (b) Vicić, D. A.; Jones, W. D. *J. Am. Chem. Soc.* **1997**, *119*, 10855.

(19) Alonso, F.; Riente, P.; Yus, M. *Synlett* **2007**, *12*, 1877.

(20) (a) *Oxford Diffraction CrysAlis CCD and CrysAlis RED*; Oxford Diffraction Ltd.: Abingdon, England, 2010. (b) Clark, C.; Ried, J. S. *Acta Crystallogr., Sect. A: Found. Crystallogr.* **1995**, *51*, 887. (c) Sheldrick, G. M. *SHELXS97 and SHELXL97*; University of Göttingen: Göttingen, Germany, 2008. (d) Farrugia, L. J. *J. Appl. Crystallogr.* **1997**, *30*, 565. (e) Farrugia, L. J. *J. Appl. Crystallogr.* **1999**, *32*, 837.